Fibers and Polymers 2014, Vol.15, No.12, 2625-2632
DOI 10.1007/s12221-014-2625-2

ISSN 1229-9197 (print version)
ISSN 1875-0052 (electronic version)

Fracture Behaviour of Biodegradable Polymer/Polyolefin-natural Fibers Ternary Composites Systems

Minhaz-Ul Haque, Ariel Stocchi[1]*, Vera Alvarez[1], and Mariano Pracella[2]

Department of Applied Chemistry and Chemical Technology, Islamic University, Kushtia 7003, Bangladesh
[1]*Composite Materials Group, Research Institute of Material Science and Technology, Engineering Faculty, National University of Mar del Plata, Mar del Plata 7600, Argentina*
[2]*Institute for Composite and Biomedical Materials, Department of Civil and Industrial Engineering, University of Pisa, Pisa 56122, Italy*

(Received March 31, 2014; Revised September 25, 2014; Accepted September 27, 2014)

Abstract: In this work, blends of MaterBi K (MBK), a starch based biodegradable polymer with polypropylene (PP), high density polyethylene (HDPE) and polystyrene (PS) were prepared in an intensive mixer PP-g-MA; HDPE-g-MA and SEBS-g-MA were incorporated at 2 wt.% to corresponding matrix respectively in order to analyze the effect of compatibilizer amount on the morphology and final properties. The composites, with 20 wt.% of alkaline treated hemp fibers, were prepared by injection molding. Fracture and water absorption of matrices and composites were studied and the effect of each component was established. Blending of the MB matrix with PP and HDPE did not raise the *Jc*, with the exception of the MB-S3 blend which has a slight improvement in fracture energy. On the other hand, the fiber incorporation to blends improves significantly the *Jc* values for all samples compared with their respective matrices. The best result was obtained for the B8-S2 blend and the B8-P2 compatibilized blend. The water absorption of equilibrium was also studied, resulting from 0.3 % to 0.9 % for the polymer blends and raises from 5 % to 7 % for the fiber reinforced blends.

Keywords: Biodegradable polymers, Natural fibers, Blends, Fracture behavior

Introduction

The amount of plastic in municipal waste streams was equal to the combined amount of metal and glass. Biodegradable materials made from renewable resources have been tested as alternatives to petroleum-based plastics [1].

Biodegradable polymers constitute a new family of polymers designed to be degraded by living organisms. In some cases recycling is impractical or not economical and this materials offer a possible alternative to traditional non-degradable polymers because they can be composted together with food and yard waste [2,3]. One of the main drawbacks of these materials is their high cost and low specific properties. An advantageous possibility is that to use blends of biodegradable polymers with traditional ones to obtain materials with improved cost/performances ratio [4,5].

In a previous paper [6] we have examined the morphology, thermal and tensile properties of binary and ternary composites founding a significant improvement of tensile modulus and strength for composites of MB with PE and PS as compared to binary MB/H composites. The results indicated that the presence of polyolefin may have a positive effect on the process-ability of the composites (higher thermal stability of ternary systems). The compatibilization of MB/PP and MB/PP/H samples by addition of PP-g-MA (2-10 wt.%) resulted in an improved phase dispersion with reduced particle size, better interfacial adhesion and significant changes in tensile properties. Moreover, nucleating effect on the crystallization of the MB matrix was also observed at the interface of polyolefin particles. It was concluded that incorporation of polyolefins in the biodegradable matrix, compared to binary matrix/fibre system, may have significant advantages in terms of properties, processability and cost.

On the other hand, the low specific gravity, the workable specific modulus, the low cost and the non-abrasive, renewable and biodegradable nature of cellulosic fibers, make them attractive to use as reinforcements in composite materials [7-11]. However, natural fiber reinforced materials have substantially inferior mechanical and water resistance properties than conventional glass fiber reinforced composites [12].

In order to improve the adhesion between cellulosic fibers and polymers, and to reduce the moisture absorption, there are several chemical treatments [13]. The alkali treatment is one of the most used and it cleans the fiber surface increases the number of free hydroxyl groups in the fiber surface, and produce changes on the chemical composition of the natural fibers (extraction of the lignin and hemicellulose) [14,15]. Moreover, depending on the treatment condition, the alkali treatment produces a rough surface; hence the number of anchorage points increases offering a good fiber-matrix mechanical interlocking [14-16].

The mechanical requirements of plastics for use in packaging may be studied by means on fracture mechanical approaches [17]. In their desire to characterize toughness of polymer composites more exactly, many researchers have turned to Fracture Mechanics [18]. In this work, the fracture behavior of biodegradable polyester/polyolefin blend composites containing natural fibers was studied under quasi-static

*Corresponding author: arstocchi@fi.mdp.edu.ar

conditions and toughness was evaluated by means of Fracture Mechanics approaches. The final objective is to obtain materials with improved mechanical properties, lower cost and reduced environmental impact.

Theoretical Background

Different fracture mechanics approaches can be applied depending on materials' behavior [19-21]. In cases where there is no significant crack growth resistance, the value of the J-integral at initiation, J_{Ic}, is a good measure of toughness. The J-integral is conventionally defined for nonlinear elastic materials as a path independent line integral. In fact, the single-specimen J formulation has been extensively used in the past to characterize the ductile fracture in polymers [19]. The *Jc* parameter is applicable to characterize the quasi-brittle failure behavior (load-displacement curves with sharp load drop at the point of fracture) of specimens with a crack to depth ratio close to 0.5. *Jc* was evaluated at the instability load point by calculating the fracture energy required to produce cleavage behavior of pre-cracked specimens having a crack depth-to-width ratio of $0.45 \le a/W \le 0.55$ as:

$$J_c = \frac{\eta U_{tot}}{S(W-a)} \tag{1}$$

where U_{tot} is the overall fracture energy, i.e., the total area under the load-deflection curve, S the thickness of tested specimens, and η a geometry factor for DENT specimens is expressed as

$$\eta = -0.06 + 5.99\left(\frac{a}{W}\right) - 7.42\left(\frac{a}{W}\right)^2 + 3.29\left(\frac{a}{W}\right)^3 \tag{2}$$

The *J*-integral approach is a natural extension of linear elastic fracture mechanics and works best for not too ductile fractures.

Otherwise a methodology that works well for very ductile polymer composites is the essential work of fracture (EWF) approach [22]. This approach was first proposed for plane stress ductile metal fractures and later applied to polymers [20].

In this work J_{Ic} was implemented, since the materials behavior fit in the method requirements.

Values of the critical stress intensity factor (K_{IC}) can be also determined from fracture mechanics. For linear elastic conditions J parameter can be taken as the energy release rate G [21] and G_{IC} can also be calculated from fracture toughness values as:

$$G_{IC} = J_c = \frac{K_{IC}^2}{E(1-\upsilon^2)} \tag{3}$$

where E is the modulus of elasticity and υ is the Poisson's ratio of the material. Since the energy release rate describes a global behavior, the critical stress intensity factor is a local parameter [23].

Experimental

Materials

A biodegradable and compostable thermoplastic, MaterBi-K (MB), based on polycaprolactone (PCL), thermoplastic starch and additives (biodegradation time under controlled conditions: 20-45 days), was kindly supplied by Novamont (Novara, Italy). Isotactic polypropylene (PP), Moplen X30S (MFR=8-10 g/10 min, *Mw*=350,000 Da and *Mn*=46,900 Da), and polypropylenegraft-maleic anhydride (PP-g-MA) (MA content 0.5-1 wt.%) were supplied by Himont and Montell, Italy, respectively. High density polyethylene (HDPE), Eltex B5920 (MFR=0.39 g/10 min) was supplied by Solvay; polystyrene (PS) powder (density=1.05 g/cm^3) was supplied by Goodfellow, England. HDPE-g-MA, Polybond 3009 (MFR=3-6 g/10 min, density=0.95 g/cm^3, MA content 4 wt.%) was supplied by Uniroyal Chemical, Italy. SEBS-g-MA, Kraton FG-1901X (MFR=22 g/10 min (200 °C, 5 kg), density=0.91 g/cm^3, MA content 2 wt.%) was supplied by Shell Chem, Italy. Hemp (Cannabis sativa) fibres were kindly supplied by Sassetti Agricoltura S.r.l. (Bientina, Italy).

In order to remove the non-cellulosic components, the fibres were first washed with liquid soap and immersed in 6 % NaOH solution for 24 h at 40 °C. The alkali treatment increases the number of free hydroxyl groups on the fiber surface and produces changes in the chemical composition by extracting lignin and hemicellulose [24]. After NaOH treatment the fibres were repeatedly rinsed with distilled water, dried at 105 °C and finally stored for use.

Blends and Composite Preparation

Blends of MaterBi K (MB) and polypropylene (PP), high density polyethylene (HDPE) and polystyrene (PS) were prepared in an intensive mixer Brabender Plasti-corder. PP-g-MA; HDPE-g-MA and SEBS-g-MA were incorporated at 2 wt.% to corresponding matrix respectively.

In order to analyze the effect of compatibilizer amount on the morphology and final properties, polypropylene-graft-maleic anhydride (PP-g-MA) was charged. First MBK was melt then compatibilizer was added and finally plain PP. Batch of 80 wt.% MBK- 20 wt.% hemp was prepared The mixing temperature and time were 175 °C and 15 min respectively. The mixing was carried out under N2 stream fixing rotor speed 60 rpm.

The composites were injected to prepare oar shape using a Proma WL-5 micro-injector. Cylinder and mold temperature were 170 °C and 50 °C respectively. The different materials obtained are listed in Table 1 with their respective nomenclature.

Fracture Tests

Fracture characterization was carried out on mode I double edge-notched tensile (DENT) specimens cut from 0.5-mm films (nominal width W was 15 mm and nominal length S was 70 mm), at a cross-head speed of 1.5 mm/min.

Table 1. Names of different obtained materials used for fracture characterization

Composition	Short name
Matrices	
MaterBi K	MB
MaterBi K 70 wt.%, polypropylene 30 wt.%	MB-P3
MaterBi K 70 wt.%, high density polyethylene 30 wt.%	MB-E3
MaterBi K 70 wt.%, high density polyethylene 30 wt.% compatibilized	MB-E3*
MaterBi K 70 wt.%, polystyrene 30 wt.%	MB-S3
MaterBi K 70 wt.%, polystyrene 30 wt.% compatibilized	MB-S3*
Composites	
Batch: MBK 80 wt.% - hemp 20 wt.%	B
Batch 80 wt.%, MaterBi K 20 wt.%	B8-MB2
Batch 80 wt.%, polystyrene 20 wt.%	B8-S2
Batch 80 wt.%, polypropylene 20 wt.%	B8-P2
Batch 80 wt.%, high density polyethylene 20 wt.%	B8-E2
Batch 80 wt.%, polystyrene 20 wt.% compatibilized	B8-S2*
Batch 80 wt.%, high density polyethylene 20 wt.% compatibilized	B8-E2*
Batch 80 wt.%, polypropylene 20 wt.% compatibilized	B8-P2*

Sharp notches were introduced by scalpel-sliding a fresh razor blade having an on-edge tip radius of 0.13 mm. Series of five specimens were tested. Critical stress intensity factor (K_{IC}) values and energy release rate values were obtained from these tests.

Water Absorption Tests

Composite applications frequently involve contact with fluids that can affect the material mechanical performance. In the particular case of water, it is well established in the literature [25] that it not only interacts with the matrix through plasticization, swelling or hydrolysis, but also attacks the interface between fiber and matrix. Small water molecules are able to diffuse into a weak fiber-matrix interface as well as to filter through matrix cracks and voids or even to migrate along the fibers by capillarity [25].

Water sorption kinetics was followed by means of gravimetric measurements on at least four specimens (0.05 g nominal weight) using an analytical balance with an accuracy of ±0.01 mg. Rectangular samples of 15 mm×10 mm×0.5 mm were cut from plaques and dried in a vacuum oven at 50 °C for 96 h. Each specimen was weighed before the water immersion. The samples were immersed in distilled water at 23 °C to determine the water absorption kinetics. The samples were blotted with tissue paper to remove the excess water on the surface, and weighted. The weight values of the dry and the sample after of water immersion were designated as W_{in} and W_{end} respectively. The value of water absorption was determined by applying the following equation:

$$\frac{(W_{end}-W_{in})}{W_{end}} \times 100 \quad (4)$$

Several measurements at different time interval were performed for each sample. The results are reported as average value. Distilled water was used, since it allows the simulation of the worst possible water damage scenario due to the lack of impurities and ions that leads a very aggressive form of moisture [26].

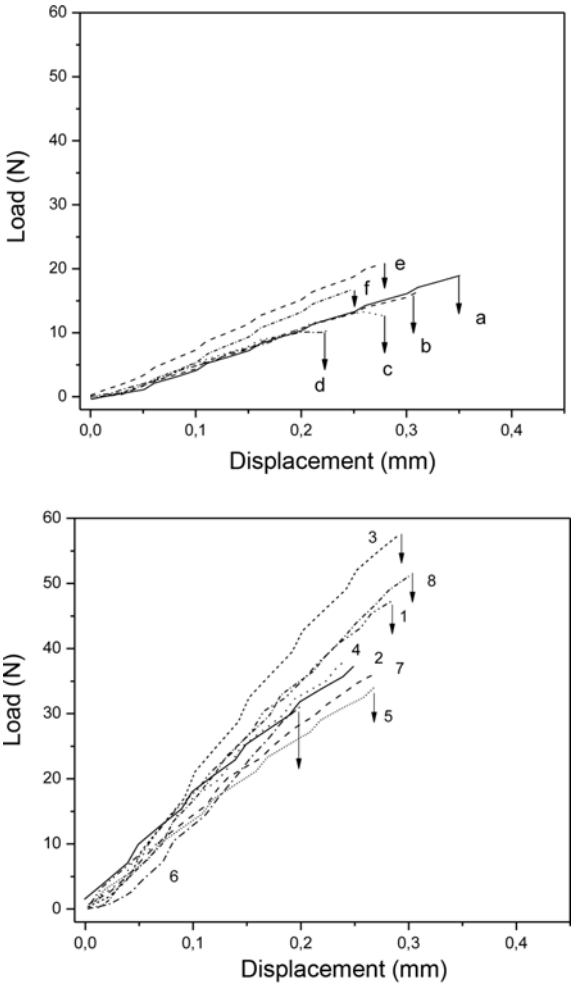

Figure 1. Load-displacement curves obtained in fracture tests formatrices and composites films; (a) MBK, (b) MB-P3, (c) MB-E3, (d) MB-E3*, (e) MB-S3, (f) MB-S3*, (1) B, (2) B8-MB2, (3) B8-S2, (4) B8-P2, (5) B8-E2, (6) B8-S2*, (7) B8-S2*, and (8) B8-P2*.

Morphological Analysis (Scanning Electron Microscopy)

Broken samples were studied by scanning electron microscopy (SEM) after they had been coated by a thin layer of gold.

Results and Discussion

Mode I Fracture Analysis of DENT Specimens

For simplicity, the materials were organized in two groups. First group (a-f) corresponds to the blends of MB with different polymer and compatibilizers; i.e, the matrices. The second group (1-8) has the blends between the batch and different polymers and compatibilizers; i.e. the composites.

Typical load-displacement curves for the films of the 2 groups (matrices and composites) are shown in Figure 1. Visual observation of the specimens during the test indicated that, in all cases, the yielding of the full ligament before crack propagation did not occurred [19]. In addition, in all cases, the crack propagation was not stable. A sharp load drop after maximum was found for all samples. So that, in order to measure the toughness of the studied materials, the J_{Ic} parameter was adopted, since some linearity of the records that evidence low plastic deformations [23].

In Figure 1(a), is possible to observe that the incorporation of PP, HDPE and compatibilizers to the biodegradable matrix did not produce an improvement in the maximum load or deformation compared with pure MB. For MB/PP blends it was found a remarkable decrease effect of PP-g-MA content on the average particle size in accordance with our previous results [6] however, this decrease in particle size did not lead to an improvement in fracture properties. There exists, however, a good correlation between the spherulite size and the fracture toughness, i.e. the larger the spherulite size is, the lower values of *Jc* measured in accordance with other authors [27].

This could be related with the low compatibility between both component, which was previously reported [6]. The weak interfacial adhesion found for almost all blends could not prevent the generation of new crack-surfaces, and the cracks can easily propagate on the interphase. Moreover, stress concentration takes place in the vicinity of the phase separations due to the difference of elastic modulus between the phases, and initiates localized micro-damages in this region. Larger second phases may induce severe stress concentrations in wider regions than smaller phases, lowering the fracture properties [28].

An effect of crystallization change on fracture properties induced by the polymer blending was expected, however the incorporation of a polyolefin into the biodegradable material produced only minor changes in the crystallization and melting behavior of MB, as a consequence of phase separation phenomena due to the lack of miscibility between the polyolefin and other polar components (i.e., polyester and starch), even if the existence of crystalline interactions have been reported for blends of PCL with polyethylene and polypropylene [29]. This behavior was also confirmed with the SEM micrographs of fracture surfaces that showed MB matrix and dispersed polyolefin (PP and PE) phase appear as separated phases, due to the immiscibility of components; displaying a characteristic droplet-like morphology with rather homogeneous size distribution as will be discussed later.

The only exception was the 30 wt.% PS (MB-S3) blend, which improves the maximum load values of Figure 1(b) shows typical load-displacement curves of natural fiber reinforced composites. As expected all materials showed higher maximum load as consequence of the fiber incorporation [30]. It can be easily seen that the curves became steeper with increased fibre content. This behavior was expected because the hemp fibre has a superior Young's modulus in comparison with the matrices.

Based on load-displacement curves, toughness was evaluated using the Fracture Mechanics approaches described in experimental section, and the results are shown in Table 2.

The J_{Ic} values obtained for unreinforced and fiber-reinforced blends are displayed in Figures 2(a) and (b) respectively. It

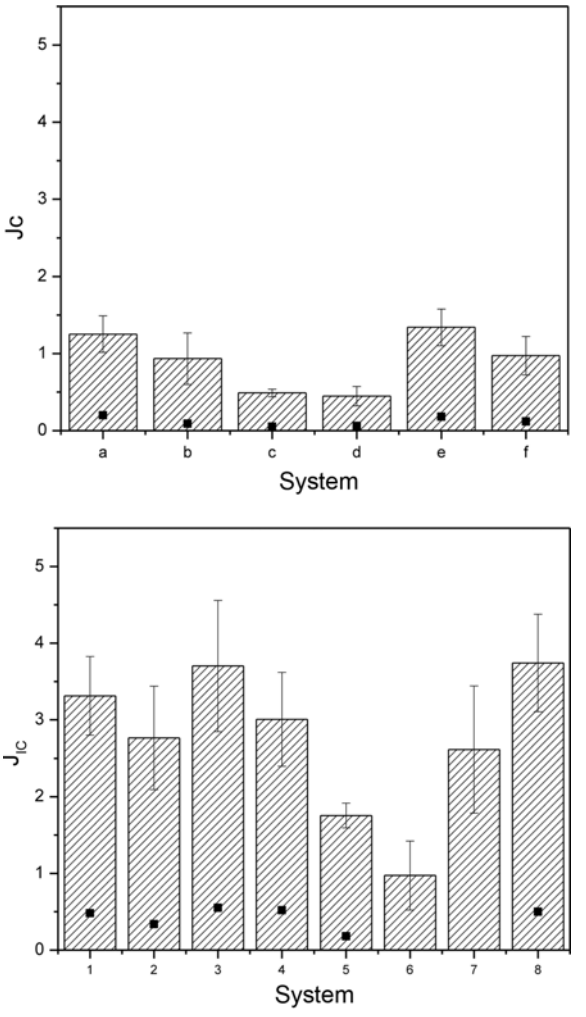

Figure 2. J_{Ic} values obtained for unreinforced (matrices) and fiber-reinforced (composites) blends; (a) MBK, (b) MB-P3, (c) MB-E3, (d) MB-E3*, (e) MB-S3, (f) MB-S3*, (1) B, (2) B8-MB2, (3) B8-S2, (4) B8-P2, (5) B8-E2, (6) B8-S2*, (7) B8-S2*, and (8) B8-P2* (the points indicates the J_{IC} calculated values).

can be clearly seen in Figure 2 that the blending of the MB matrix with PP and HDPE did not raise the J_c, with the exception of the MB-S3 blend which has a slight improvement in fracture energy, probably due to a better compatibility among the other blends. On the other hand, the fiber incorporation to blends improves significantly the J_c values for all samples compared with their respective matrices. The best result was obtained for the B8-S2 (3 in Figure 2(b)) blend and the B8-P2 compatibilized blend (8 in Figure 2(b)). These results are in concordance with the mechanical results (tensile strength and Young's modulus) obtained in a previous work [4], were the best mechanical properties were found for the MB-S3 blend and the B8-S2 fiber reinforced blend. The strength of MB/PS results to be higher than that of MB/PP and MB/PE. The incorporation of 32 wt.% fibres into MB (MB/H) caused a marked rise of the modulus. It was also observed in that work that the addition of compatibilizers (2 wt.%) did not induce significant changes on the tensile properties [4].

Values of the critical stress intensity factor (K_{IC}) were also determined from load-displacement curves (Figure 1). For linear elastic conditions J parameter can be taken as G [21] and G_{IC} can also be calculated from fracture toughness values as showed in equation (3). The Poisson's ratio of the polymer, was taken to be 0.4 in accordance with the literature [31].

The results of the above calculation showed differences among the calculated and the measured values of the energy release rate parameter. These values can be seen in Figure 2 as points. Values being measured values always higher than calculates ones. This is probably due to the existence of energy dissipation mechanisms, such as plastic void growth and matrix plastic deformation, that are not accounted in LEFM [32]. In all cases the calculated values follow the trend of the measured energy release rate parameter.

It is important to note that the incorporation of compatibilizer in blends of MB and High density polyethylene, pure and reinforced with fibers improved the K_{IC} values. In that particular case it can be concluded that an improvement in the interphase between polymers and with the fibers could be attained.

Fracture Surface Analysis

In order to analyze the failure mechanisms operative in the investigated materials, SEM was performed on the fracture surfaces of samples broken during fracture tests.

The toughness of unreinforced and fiber-reinforced blends can be explained by means of several sources of energy dissipation processes such as, fracture of matrix or fibers, debonding and cavitation of second phases, crazing and shear yielding of the matrix, fiber-matrix debonding, fiber fracture, axial fiber splitting and fiber pull-out [33,34].

Figure 3(a) shows the aspect of the MB fracture surface. A particular structure for the pure Mater-Bi with granules distributed within a continuous phase was found accordingly to the literature [35]. It can be seen that the dispersed phase consists of plasticized starch in the form of droplet-like particles. In such micrography no evidence of extensive plastic deformation was found.

The MB-P3 blend exhibited a characteristic droplet-like morphology with rather homogeneous size distribution

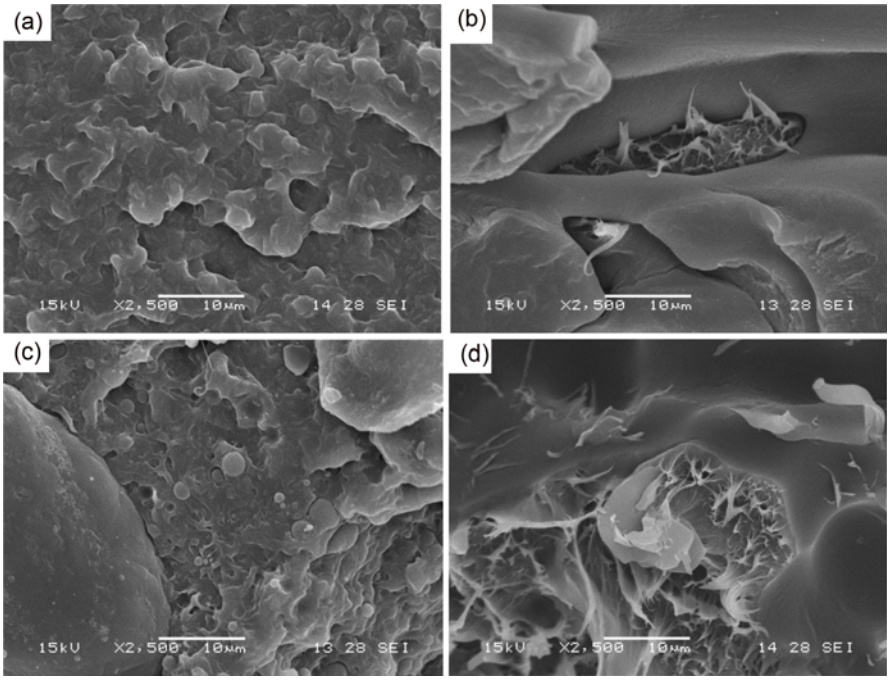

Figure 3. SEM micrograph of fracture surfaces of; (a) MB, (b) MB-P3, (c) MB-E3, and (d) MB-S3.

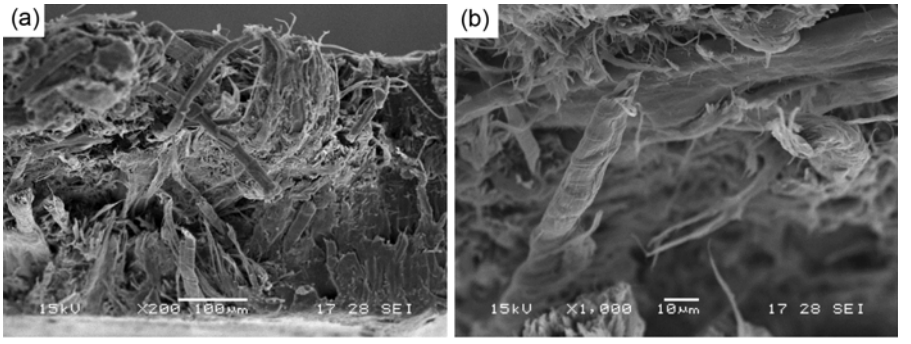

Figure 4. SEM micrograph of fracture surfaces of batch (B) at different magnifications; (a) 200× and (b) 1000×.

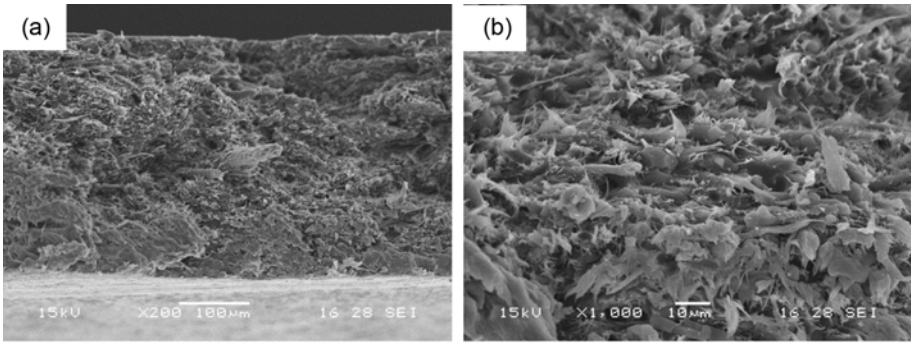

Figure 5. SEM micrograph of fracture surfaces of MB-8S blend at different magnification; (a) 200× and (b) 1000×.

(Figure 3(b)), and a similar morphology was observed for MB-E3 with larger second PE domains with low plastic deformations (Figure 3(c)). In all cases immiscibility of components was found [4]. The lower fracture energy of the blend compared with the pure MB can be explained as the second phase acted as a defect due the low compatibility between the components leading to a decrease in fracture parameters [18]. Moreover in the case of MB-P3 (Figure 3(b)) and MB-S3 (Figure 3(d)) it can be observed high heterogeneous plastic deformations between the two components indicating that the plastic flow of one of the components starts at lower stresses than the yield strength of the matrix. This effect was already observed by Tuba *et al.* [18] for PLA/PCL blends.

The aspect of the fracture surface of MB-S3 blend is showed in Figure 3(d). It is easy to see that better compatibility between PS and MB was attained leading to smaller second phase domains and thus lesser stress concentrations. Also plastic deformation of the PS is present, resulting in an increment in the fracture energy. The blends with compatibilizer showed smaller second phase domains in all cases; however it is possible to see worst interfacial adhesion, leading to lower fracture properties.

Figure 4(a) shows the fracture surface of the batch sample. As it can be observed in that figure, Batch of MB (B) and hemp fibers presents entire yarn pull out and individual fiber pull out of fiber oriented parallel to loading direction. In the case of fibers perpendicular to the loading direction fiber pullout appears to be suppressed. The fibers deform and break up locally. This is associated with stress release and stress redistribution processes, leading to improved fracture energy.

As a consequence of the fiber incorporation, a larger damage zone is present in fiber reinforced composites compared with unreinforced blends. The energy dissipation is higher not only as a consequence of fiber related energy dissipating mechanisms (debonding, pull-out and fracture) the larger extension of damage zone plays an important factor in the improvement of fracture energy [34].

Closer view (Figure 4(b)), shows the main failure mechanisms of the investigated batch found. Complete yarn pull-out, partial untwisting of the yarns, individual fiber pull out, axial splitting and defibrillation corresponding to relatively low adhesion between matrix and fibers can be clearly seen in this figure [36-38]. In general, a number of mechanisms contribute to the fracture toughness and it is often very difficult to determine the dominant mechanism [39].

Views of the MB-8S blend are presented in Figure 5(a). It is possible to see that the pull-out length was notably shorter than that for the batch alone. In addition closer views of the MB-8S (Figure 5(b)) blend also shows fiber breakage and improved matrix-fiber adhesion evidenced by material added to

Table 2. Fracture parameters of matrices and composites

Sample	J_{Ic} (J/m^2) (measured)	E (MPa)[6]	K_{Ic} (MPa·m$^{1/2}$) (measured)
Matrices			
MB	1.25±0.24	440.2±46.3	0.32±0.09
MB-P3	0.93±0.33	640.8±70.3	0.26 ±0.04
MB-E3	0.49±0.05	484.2±24.6	0.17±0.01
MB-E3*	0.45±0.13	475.8±23.5	0.18±0.02
MB-S3	1.34±0.24	751.1±25.8	0.40±0.04
MB-S3*	0.97±0.27	717.3±40.7	0.32±0.07
Composites			
B	3.31±0.51	1406.0±38.1	0.89±0.09
B8-MB2	2.77±0.67	1272.9±57.8	0.71±0.07
B8-S2	3.70±0.86	1582.2±72.2	1.01±0.09
B8-P2	3.01±0.61	1360.7±44.7	0.91±0.06
B8-E2	1.75±0.16	1567.9±73.6	0.58±0.02
B8-S2*	0.97±0.45	nd	0.66±0.02
B8-E2*	2.61±0.83	nd	0.68±0.09
B8-P2*	3.74±0.64	1115.0±70.0	0.81±0.09

Table 3. Equilibrium water content of matrices and composites

Matrices		Composites	
Material	Water uptake at equilibrium (%)	Material	Water uptake at equilibrium (%)
MB	0.38±0.12	B	5.51±0.92
MB-P3	0.42±0.23	B8-MB2	7.03±0.04
MB-E3	0.31±0.10	B8-S2	4.79±0.05
MB-E3*	0.94±0.05	B8-P2	6.82±1.53
MB-S3	0.56±0.14	B8-E2	6.28±0.09
MB-S3*	0.37±0.25	B8-S2*	6.19±0.27
		B8-E2*	5.26±0.59

the debonded fiber surface [36-38].

Water Absorption

Water absorption is one of the main shortcomings that restrict the application of starch-based materials [40]. The water absorption in these materials seriously reduces the mechanical properties [40,41]. The results of water absorption tests are shown in Table 3 for the blends and composites.

The water absorption of equilibrium of the unreinforced materials was low, ranging from 0.3 % to 0.9 % for the polymer blends. These values raised from 5 % to 7 % for the fiber reinforced blends. Water absorbed in the materials can be free water and bound water [8]. Water molecules contained in the free volume of polymer, micro-voids and holes are identified as free water. Water molecules that are dispersed in the polymer-matrix and attached to the polar groups of the polymer are designated as bound water [42]. The good consolidation and the low void content observer for the unreinforced blends indicates that the measured water absorption was mainly bound water. On the other hand, with the fiber incorporation, water can penetrate into the cellulose network of the reinforcement and into the capillaries and spaces between the fibrils and the fiber-matrix interphase. Water can also attach itself by chemical links to groups in the cellulose molecules of the hemp fibers. All these factors explain the higher contents water uptake at equilibrium found for the fiber reinforced blends.

This water absorption behavior is one of the most significant drawbacks on the fiber incorporation, however the improvement of the mechanical properties leads to a balance of this two factors for each particular application [43].

It was observed that the time for equilibrium was near to 30 h in all cases. Future works regarding the effect of water absorption on the mechanical behavior of studied materials are being carried out.

Conclusion

In the present work, the deformation, fracture and water absorption of MaterBi K blends were investigated. Special emphasis was put in the identification of the toughening mechanisms operative in these materials. Fracture characterization was carried out on mode I double edge-notched tensile (DENT). Evidence low plastic deformations were observed. The blending of the MB matrix with PP and HDPE did not raise the J_{Ic}, with the exception of the MB-S3 blend which has a slight improvement in fracture energy. On the other hand, the fiber incorporation to blends improves significantly the J_{Ic} values for all samples compared with their respective matrices. The best result was obtained for the B8-S2 blend and the B8-P2 compatibilized blend. From the SEM analysis performed on the fracture surfaces, no evidence of extensive plastic deformation was found in the case of MB samples. The blends with PP, PE and PS exhibited a characteristic droplet-like morphology with rather homogeneous size distribution. In all cases immiscibility of components was found. From the fracture surface of the batch sample, yarn pull-out, partial untwisting of the yarns and individual fiber pull out and defibrillation corresponding to relatively low adhesion between matrix and fibers was observed. In all cases the incorporation of fibers enhances the mechanical performance of the blends, resulting in a reduction of the matrix material that lowers the cost of the material and reduces the environmental impact of the disposal of these materials at their end of life cycle.

The water absorption of equilibrium was from 0.3 % to 0.9 % for the polymer blends and raises from 5 % to 7 % for the fiber reinforced blends. Future works regarding the effect of water absorption on the mechanical behavior of studied materials are being carried out.

Acknowledgments

Authors acknowledged ANPCyT (Fonarsec FSNano004), CNR-CONICET (Cooperation Agreement between CNR, Italy and CONICET, Argentina 2013-2014) and UNMdP for the financial support.

References

1. Q. Fang and M. A. Hanna, *Ind. Crops. Prod.*, **13**, 219 (2001).
2. G. Doyon, J. Arch, D. Twede, B. Drasner, A. M. Baylis, D. R. Kopsilk, E. Fisher, F. J. Sweeney, M. W. Leonard, B. Finnigan, L. Liu, J. Kost, P. Takhistov, C. Irwin, A. S. Mandel, G. A. Foster, L. Lynch, R. M. Brasington, R. Quinn, and P. Henningsen, "The Wiley Encyclopedia of Packaging Technology", John Wiley & Sons Inc., 2010.
3. H.-S. Kim and H.-J. Kim, *Fiber. Polym.*, **14**, 793 (2013).
4. I. Vroman and L. Tighzert, *Materials*, **2**, 307 (2009).
5. K. Song and I. Kim, *Fiber. Polym.*, **14**, 2135 (2013).
6. M. M.-U. Haque, V. Alvarez, M. Paci, and M. Pracella, *Compos. Part A-Appl. S.*, **42**, 2060 (2011).
7. P. Wambua, J. Ivens, and I. Verpoest, *Compos. Sci. Technol.*, **63**, 1259 (2003).
8. A. Stocchi, C. Bernal, A. Vázquez, J. Biagotti, and J. Kenny, *J. Compos. Mater.*, **41**, 2005 (2007).
9. S. Nam and A. Netravali, *Fiber. Polym.*, **7**, 380 (2006).
10. K. Leluk and M. Kozlowski, *Fiber. Polym.*, **15**, 108 (2014).
11. A. Ibrahim, M. V. Wahit, and A. A. Yussuf, *Fiber. Polym.*, **15**, 574 (2014).
12. S. H. Aziz and M. P. Ansell, *Compos. Sci. Technol.*, **64**, 1231 (2004).
13. C. Vallo, J. M. Kenny, A. Vazquez, and V. P. Cyras, *J. Compos. Mater.*, **38**, 1387 (2004).
14. L. Y. Mwaikambo and M. P. Ansell, *J. Appl. Polym. Sci.*, **84**, 2222 (2002).
15. J. A. Khan, M. A. Khan, and R. Islam, *Fiber. Polym.*, **13**, 1300 (2012).
16. K. Mahato, S. Goswami, and A. Ambarkar, *Fiber. Polym.*, **15**, 1310 (2014).
17. W. Y. F. Chan and J. G. Williams, *Polymer*, **35**, 1666 (1994).
18. F. Tuba, L. Oláh, and P. Nagy, *Eng. Fract. Mech.*, **78**, 3123 (2011).
19. E. Plati and J. G. Williams, *Polym. Eng. Sci.*, **15**, 470 (1975).
20. B. Cotterell and J. K. Reddel, *Int. J. Fract.*, **13**, 267 (1977).
21. Y.-W. Mai and P. Powell, *J. Polym. Sci. Part B-Polym. Phys.*, **29**, 785 (1991).
22. J. Karger-Kocsis, T. Czigány, and E. J. Moskala, *Polymer*, **38**, 4587 (1997).
23. T. L. Anderson, "Fracture Mechanics: Fundamentals and Applications", CRC Press, Boca Ratón, Florida, USA, 2005.
24. J. Gassan and A. K. Bledzki, *Compos. Sci. Technol.*, **59**, 1303 (1999).
25. J.-K. Kim and Y.-W. Mai in "Engineered Interfaces in Fiber Reinforced Composites" (J.-K. Kim and Y.-W. Mai Eds.), pp.1-4, Elsevier Science Ltd., Oxford, 1998.
26. F. Ellyin and R. Maser, *Compos. Sci. Technol.*, **64**, 1863 (2004).
27. L. Ye, A. Beehag, and K. Friedrich, *Compos. Sci. Technol.*, **53**, 167 (1995).
28. M. Todo, S. D. Park, T. Takayama, and K. Arakawa, *Eng. Fract. Mech.*, **74**, 1872 (2007).
29. D. R. Paul, "Polymer Blends", Elsevier, 1978.
30. K. L. Pickering, M. A. Sawpan, J. Jayaraman, and A. Fernyhough, *Compos. Part A-Appl. S.*, **42**, 1148 (2011).
31. S. S. Lawrence, P. S. Walia, F. Felker, and J. L. Willett, *Polym. Eng. Sci.*, **44**, 1839 (2004).
32. A. Stocchi, E. Rodríguez, A. Vázquez, and C. Bernal, *J. Appl. Polym. Sci.*, **128**, 1547 (2013).
33. S. C. Tjong, S.-A. Xu, R. K.-Y. Li, and Y.-W. Mai, *Compos. Sci. Technol.*, **62**, 831 (2002).
34. J. Karger-Kocsis, T. Harmia, and T. Czigány, *Compos. Sci. Technol.*, **54**, 287 (1995).
35. R. Moriana, F. Vilaplana, S. Karlsson, and A. Ribes-Greus, *Compos. Part A-Appl. S.*, **42**, 30 (2011).
36. T. Harmia and K. Friedrich, *Compos. Sci. Technol.*, **53**, 423 (1995).
37. R. V. Silva, D. Spinelli, W. W. Bose Filho, S. Claro Neto, G. O. Chierice, and J. R. Tarpani, *Compos. Sci. Technol.*, **66**, 1328 (2006).
38. V. Alvarez, A. Vazquez, and C. Bernal, *J. Compos. Mater.*, **40**, 21 (2006).
39. F. L. Matthews and R. D. Rawlings, "Composite Materials: Engineering and Science", Elsevier, 1999.
40. H. Ma and C. W. Joo, *Fiber. Polym.*, **12**, 310 (2011).
41. J.-B. Zeng, L. Jiao, Y.-D. Li, M. Srinivasan, T. Li, and Y.-Z. Wang, *Carbohydr. Polym.*, **83**, 762 (2011).
42. H. N. Dhakal, Z. Y. Zhang, and M. O. W. Richardson, *Compos. Sci. Technol.*, **67**, 1674 (2007).
43. N. Venkateshwaran and A. Elaya Perumal, *Fiber. Polym.*, **13**, 907 (2012).